Ultra-broad near-infrared emission of Bi-doped $SiO_2-Al_2O_3-GeO_2$ optical fibers

Jindong Wu (吴金东)[1,3*], Danping Chen (陈丹平)[2], Xingkun Wu (吴兴坤)[1], and Jianrong Qiu (邱建荣)[4,5]**

[1]*State Key Laboratory of Modern Instruments, Department of Optical Engineering, Zhejiang University, Hangzhou 310027, China*

[2]*Shanghai Institute of Optics and Fine Mechanics, Chinese Academy of Sciences, Shanghai 201800, China*

[3]*Zhejiang Futong Optical Fiber Technology Corp. Ltd., Fuyang 311422, China*

[4]*State Key Laboratory of Silicon Materials, Zhejiang University, Hangzhou 310027, China*

[5]*Optical Communication Materials Laboratory, South China University of Technology, Guangzhou 510640, China*

[*]*Corresponding author: wjd3699@sina.com;* [**]*corresponding author: qjr@zju.edu.cn*

Received December 22, 2010; accepted March 3, 2011; posted online May 12, 2011

Bi-doped SiO_2–Al_2O_3–GeO_2 fiber preforms are prepared by modified chemical vapor deposition (MCVD) and solution doping process. The characteristic spectra of the preforms and fibers are experimentally investigated, and a distinct difference in emission between the two is observed. Under 808-nm excitation, an ultra-broad near-infrared (NIR) emission with full-width at half-maximum (FWHM) of 495 nm is observed in the Bi-doped fiber. This observation, to our knowledge, is the first in this field. The NIR emission consists of two bands, which may be ascribed to the Bi^0 and Bi^+ species, respectively. This Bi-doped fiber is promising for broadband optical amplification and widely tunable laser.

OCIS codes: 160.2540, 060.2390, 160.4670, 160.3380.

doi: 10.3788/COL201109.071601.

In 2001, Fujimoto *et al.* discovered a new gain material based on Bi-doped silica glass with a luminescence bandwidth of 300 nm in the optical communication window[1], and demonstrated optical amplification at 1300 nm upon 800-nm pumping[2]. Efficient gain media compatible with Si-based telecommunication fibers are scarce in the second optical communication band window, even in longer wavelength regions. Thus, the peculiar luminescence property of Bi-doped silica glass has caught considerable attention because of its role in the development of ultra-wide-band (UWB) fiber amplifier and tunable fiber laser. Recently, a series of Bi-doped host materials including silicate, germinate, phosphate, and barium borate glasses was prepared by normal melting-quenching method[3−14]. Extensive investigations on the near-infrared (NIR) luminescence properties of Bi-doped glasses have also been conducted to clarify the luminescence mechanism. Qiu *et al.*[15−17] suggested that the broadband NIR emission band was caused by Bi with low valence state, e.g., Bi^+ ions. Peng *et al.*[18] ascribed the NIR emission band to the Bi^0 species. In addition, Bi^{5+} ionic species[1], Bi_2 and Bi_2^- clusters[7,19], BiO molecules[9], and structures of the $\{[AlO_{4/2}]^-, Bi^+\}$ type[20] were proposed as activated centers by other researchers. However, the nature of Bi-related luminescent centers has not been clearly identified and thus needs further investigation.

Bi-doped silica-based fibers fabricated using modified chemical vapor deposition (MCVD) technique is regarded as a promising candidate for the development of novel fiber laser and UWB fiber amplifier[20−28]. Recently, Razdobreev *et al.*[29,30] studied the NIR emission properties of MCVD preforms and fibers with Bi-doped SiO_2–Al_2O_3–GeO_2–P_2O_5 or SiO_2–GeO_2–P_2O_5 glass as core. A significant change of the 1.3–μm luminescence property was observed between preforms and fibers. In spite of this, clarifying the mechanism of the luminescence change is still necessary. More investigations on the dependence of the NIR emission properties of glass composition variation and fabrication condition may provide new insight into the nature of Bi-related luminescence. Based on our previous work[31], a Bi-doped preform with core compositions of SiO_2–Al_2O_3–GeO_2 was fabricated with proper O_2 atmosphere and Ge-codoped concentration. An ultra-broad NIR emission with a full-width at half-maximum (FWHM) of 495 nm was observed in the Bi-doped SiO_2–Al_2O_3–GeO_2 fibers.

The preforms were prepared by MCVD and solution-doping techniques[32]. Cladding layers of SiO_2-GeO_2-F were deposited on the inner surface of a silica tube, followed by a germanosilicate soot layer with designed GeO_2 concentration. Subsequently, the layers were infiltrated with $BiCl_3$ and $AlCl_3$ hydrochloric solution. Finally, the porous soot layer absorbed with the $BiCl_3$ and $AlCl_3$ was consolidated into a transparent glassy core layer at around 1,800 °C, followed by a tube collapsing into a preform at 2,200 °C by hydrogen flame heating in an O_2-containing atmosphere. The refractive index profile of the fabricated preforms was tested using a preform profiler (PK2600, Photon Kinetics, USA). Specimens were taken from each preform by cutting into a 1-cm-thick slice for measurement, both sides of which were optically polished. Optical fibers were drawn from the preform by normal fiber drawing facilities (graphite furnace filled with argon gas) with core and outer diameters controlled at 10 and 125 μm, respectively. The NIR emission spectrum of the preform under 808-nm excitation was recorded using a spectrofluorometer (SBP300, Zolix, China). An InGaAs diode was used as detector in the 850−1,700 nm range at a resolution of 1 nm. The absorption transmission spectrum from the preform was measured using a spectrometer (QE-65000, Ocean

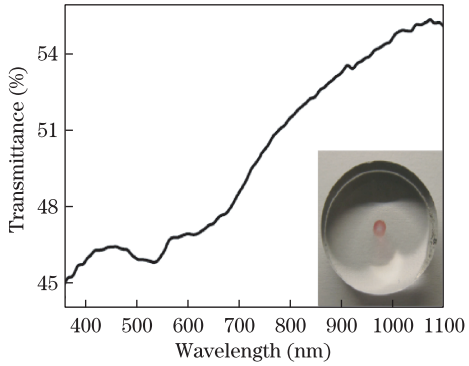

Fig. 1. Absorption spectrum of the preform. The inset is an end view of preform.

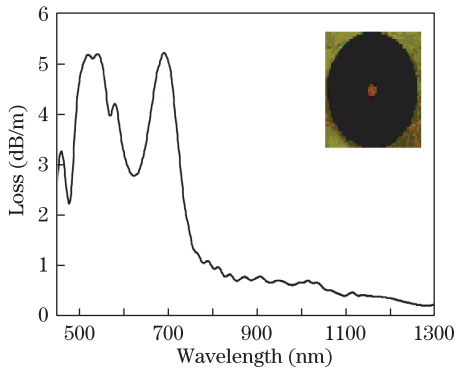

Fig. 2. Loss spectrum of the fiber. The inset is a microscopic view of the end surface of the fiber.

Optics, USA) under a 5-W xenon lamp excitation. On the other hand, the loss spectrum of the investigated fiber was measured using an optical spectrum analyzer (AQ6315A, Ando, Japan). The NIR emission spectra of the fiber were recorded using an optical spectrum analyzer (8163B, Agilent, USA) under either 808- or 976- nm pumping.

The concentrations of Bi_2O_3 and Al_2O_3 doped in the preform core were estimated by measuring Bi and Al concentrations in solution before and after soaking using inductively coupled plasma mass spectrometry. The values were approximately 0.04 and 2.63 mol%, respectively. Absorption spectrum and an end view of the preform are shown in Fig. 1. Two absorption bands located at 540 and 680 nm and a shoulder located within the 800−1,000 nm range are observed. The core of the preform shows a light crimson color. For comparison, optical loss spectrum and a microscopic view of the end surface of the fiber are shown in Fig. 2. The optical loss spectrum exhibits four characteristic absorption bands at 450, 530, 580, and 700 nm, and a shoulder locates within the 800−1,050 nm range. The fiber optical loss spectrum is slightly different from that of the preform.

Figure 3(a) shows the normalized luminescence spectra of the preform with 808-nm excitation and the fiber with 808- and 976-nm excitations. The luminescence spectrum of the preform shows an emission band at 1,276 nm with FWHM of 374 nm under 808-nm pumping. In our experiments, no luminescence from the preform was recorded under 976-nm excitation. Under 808-nm pumping, an ultra-broad emission band with FWHM of

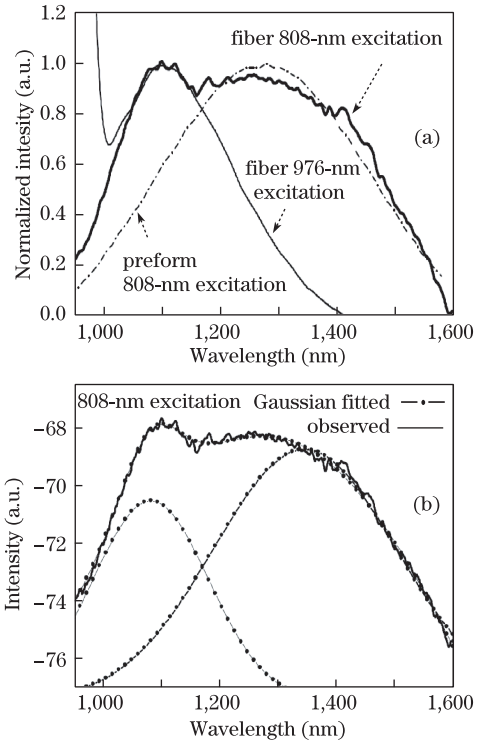

Fig. 3. Luminescence spectra of the preform and fiber: (a) preform excited at 808 nm, fiber excited at 808 and 976 nm; (b) fiber excited at 808 nm with Gaussian fitting.

495 nm was detected, which was considerably wider than that from the preform. To the best of our knowledge, this broad emission band has not been reported in Bi-doped $SiO_2-Al_2O_3-GeO_2$ fiber. The luminescence property was comparable to what had been found in Bi-doped $Li_2O-Al_2O_3-SiO_2$ glass[33] where an ultra-broad emission band with FWHM of 500 nm was detected. When excited at 976 nm, the fiber showed an emission band with a peak at 1,110 nm.

In Fig. 3(b), the emission spectrum from the fiber upon 808-nm excitation can be fitted by the two Gaussian peaks positively, peaking at 1,082 nm (with FWHM of 198 nm) and 1,345 nm (with FWHM of 312 nm). The intensities of the two emission peaks are comparable to each other, which significantly broadens the emission bandwidth.

A distinct difference in emission spectrum has been observed between preform and fiber. The emission band around 1,100 nm is not observable in the corresponding preform under 808- and 976-nm excitations. This phenomenon indicates that a new luminescent center is created during the fiber drawing process. In addition, note that the two Gaussian peaks are similar to that of the preform under 808-nm pumping and fiber under 976-nm pumping. The results suggest the existence of at least two different NIR luminescent centers in the Bi-doped fiber, one contributes to the emission at 1,100 nm while the other contributes to the emission at 1,300 nm.

Although the detailed mechanism remains unknown, the variation of luminescent properties could clearly be ascribed to different Bi-associated active centers related to the valence state of Bi or local environments around

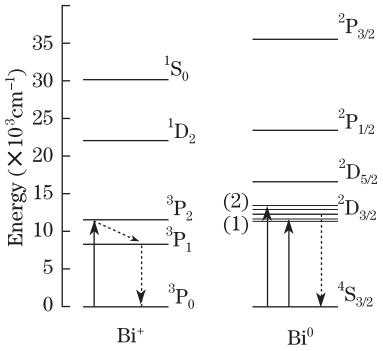

Fig. 4. Schematic energy level diagrams of Bi^+ and Bi^0 centers.

Bi ions. The NIR luminescence center might be caused by the low valence state species of Bi, such as Bi^+ or Bi^0. The schematic energy level diagrams for various Bi valence states are depicted in Fig. 4. In the present study, the NIR band at 1,100 nm matches well with the proposed energy levels of Bi^0 by Peng *et al.*[34] and could be attributed to $^2D_{3/2} \rightarrow {}^4S_{3/2}$ transition (Fig. 4). The NIR band at 1,276 nm matches well with the energy levels of Bi^+ by Qiu *et al.*[15]. This luminescent phenomenon can be understood fully with the energy diagram[16,18] in Fig. 4. The emission from the preform may be due to the Bi^+ species. When excited by 808–nm laser diode, Bi^+ is excited to $^3P_2$ and the emission around 1,276 nm ($^3P_1$ to $^3P_0$) is observed from the Bi^+. In the fiber drawing process, Bi ions underwent further annealing process at high temperature (approximately 2,200 °C) in an oxygen-free condition. Consequently, the ions partially deoxidized to Bi^0 atoms. Therefore, when the Bi^0 atom is excited at approximately 976 nm, the Bi^0 is excited to $^2D_{3/2}(1)$ state, resulting in the emission approximately 1,100 nm from Bi^0. Emissions from both Bi^0 and Bi^+ can be detected at 1,100 and 1,276 nm, respectively, because the levels of $^3P_2$ and $^2D_{3/2}(1)$ partly overlap when excited at 808 nm.

According to the observed NIR emission behavior and the energy diagram in Fig. 4, it is reasonable to assume that by selecting pumping source and configuration accurately[35] and using optical circulator and tunable fiber grating[36], one can develop widely tunable laser and wideband amplifier using the Bi-doped silica fiber.

In conclusion, a distinct difference in emission between preform and fiber is observed, implying that there are at least two types of Bi-associated emission centers in the fiber, i.e., Bi^0 and Bi^+ species. Under 808-nm excitation, an ultra-broad NIR emission with FWHM of 495 nm is achieved in the Bi-doped $SiO_2-Al_2O_3-GeO_2$ fiber, an achievement which, to our knowledge, is the first in this field. This emission consists of two bands, which may be ascribed to Bi^+ and Bi^0. The emission band at 1,100 nm could be due to the $^2D_{3/2}(1) \rightarrow {}^4S_{3/2}$ of Bi^0 and the 1,300-nm band due to the $^3P_1 \rightarrow {}^3P_0$ of Bi^+ transitions. The Bi-doped fibers are promising gain-medium candidates for broadband amplifier and widely tunable laser source.

The authors acknowledge the generous help of G. Zhang for fiber drawing, and Q. Zhou, Q. Zhang, and Y. Wei for several measurements.

References

1. Y. Fujimoto and M. Nakatsuka, Jpn. J. Appl. Phys. **40,** L279 (2001).
2. Y. Fujimoto and M. Nakatsuka, Appl. Phys. Lett. **82,** 3325 (2003).
3. M. Peng, J. Qiu, D. Chen, X. Meng, I. Yang, X. Jiang, and C. Zhu, Opt. Lett. **29,** 1998 (2004).
4. M. Peng, X. Meng, J. Qiu, Q. Zhao, and C. Zhu, Chem. Phys. Lett. **403,** 410 (2005).
5. X. Meng, J. Qiu, M. Peng, D. Chen, Q. Zhao, X. Jiang, and C. Zhu, Opt. Express **13,** 1628 (2005).
6. B. Denker, B. Galagan, V. Osiko, S. Sverchkov, and E. Dianov, Appl. Phys. B **87,** 135 (2007).
7. B. Denker, B. Galagan, V. Osiko, I. Shulman, S. Sverchkov, and E. Dianov, Appl. Phys. B **95,** 801 (2009).
8. Q. Qian, Q. Zhang, G. Yang, Z. Yang, and Z. Jiang, J. Appl. Phys. **104,** 043518 (2008).
9. J. Ren, L. Yang, J. Qiu, D. Chen, X. Jiang, and C. Zhu, Solid State Commun. **140,** 38 (2006).
10. M. Peng, J. Qiu, D. Chen, X. Meng, and C. Zhu, Opt. Lett. **30,** 2433 (2005).
11. J. Ren, J. Qiu, D. Chen, C. Wang, X. Jiang, and C. Zhu, J. Mater. Res. **22,** 1954 (2007).
12. X. Meng, J. Qiu, M. Peng, D. Chen, Q. Zhao, X. Jiang, and C. Zhu, Opt. Express **13,** 1635 (2005).
13. M. Peng, C. Wang, D. Chen, J. Qiu, X. Jiang, and C. Zhu, J. Non-Cryst. Solids **351,** 2388 (2005).
14. M. Peng, J. Qiu, D. Chen, X. Meng, and C. Zhu, Opt. Express **13,** 6892 (2005).
15. J. Qiu, M. Peng, J. Ren, X. Meng, X. Jiang, and C. Zhu, J. Non-Cryst. Solids **354,** 1235 (2008).
16. S. Zhou, N. Jiang, B. Zhu, H. Yang, S. Ye, G. Lakshminarayana, J. Hao, and J. Qiu, Adv. Funct. Mater. **18,** 1407 (2008).
17. J. Ren, G. Dong, S. Xu, R. Bao, and J. Qiu, J. Phys. Chem. A **112,** 3036 (2008).
18. M. Peng, C. Zollfrank, and L. Wondraczek, J. Phys. Condens. Matter **21,** 285106 (2009).
19. V. O. Soklov, V. G. Plotnichenko, and E. Dianov, Opt. Lett. **33,** 1488 (2008).
20. V. V. Dvoyrin, V. M. Mashinsky, E. M. Dianov, A. A. Umnikov, M. V. Yashkov, and A. N. Guryanov, in *Proceedings of 31st European Conference on Optical Communication* **4,** 949 (2005).
21. E. M. Dianov, V. V. Dvoyrin, V. M. Mashinsky, A. A. Umnikov, M. V. Yashkov, and A. N. Gur'yanov, Quant. Electron. **35,** 1083 (2005).
22. Y.-S. Seo, Y. Fujimoto, and M. Nakatsuka, in *Proceedings of CLEO/QELS* CTuI6 (2006).
23. V. V. Dvoyrin, V. M. Mashinsky, E. M. Dianov, A. A. Umnikov, M. V. Yashkov, and A. N. Guryanov, in *Proceedings of OFC/NFOEC 2006* OTuH4 (2006).
24. E. M. Dianov, S. V. firstov, V. F. Khopin, A. N. Guryanov, and I. A. Bufetov, Quant. Electron. **38,** 615 (2008).
25. I. A. Bufetov, S. V. firstov, V. F. Khopin, O. I. Medvedkov, A. N. Guryanov, and E. M. Dianov, Opt. Lett. **33,** 2227 (2008).
26. V. V. Dvoyrin, O. I. Medvedkov, V. M. Mashinsky, A. A. Umnikov, A. N. Guryanov, and E. M. Dianov, Opt. Express **21,** 16971 (2008).
27. E. M. Dianov, S. V. firstov, O. I. Medvedkov, I. A. Bufetov, V. F. Khopin, and A. N. Guryanov, in *Proceedings*

of OFC 2009 OWT3 (2009).

28. A. A. Umnikov, A. N. Guryanov, A. N. Abramov, N. N. Vechkanov, S. V. firstov, V. M. Mashinsky, V. V. Dvoyrin, L. I. Bulatov, and E. M. Dianov, in *Proceedings of ECOC 2008* Tu.1.B.7 (2008).
29. I. Razdobreev, L. Bigot, V. Pureur, A. Favre, G. Bouwmans, and M. Douay, Appl. Phys. Lett. **90,** 031103 (2007).
30. V. G. Truong, L. Bigot, A. Lerouge, M. Douay, and I. Razdobreev, Appl. Phys. Lett. **92,** 041908 (2008).
31. J. Wu, D. Chen, W. Lu, L. Zhang, X. Wu, and J. Qiu, Acta Opt. Sin. (in Chinese) **31,** 0406003 (2011).
32. G. Chen, Y. Li, Y. He, L. Liu, L. Xu, and W. Wang, Chin. Opt. Lett. **7,** 348 (2009).
33. T. Suzukia and Y. Ohishi, Appl. Phys. Lett. **88,** 191912 (2006).
34. M. Peng, B. Sprenger, M. A. Schmidt, H. G. L. Schwefel, and L. Wondraczek, Opt. Express **18,** 12852 (2010).
35. J. Wang, L. Yin, X. Shi, X. Ma, L. Li, and X. Zhu, Chin. Opt. Lett. **8,** 591 (2010).
36. Y. Shen, C. Gu, L. Xu, A. Wang, H. Ming, Y. Liu, and X. Wang, Chin. Opt. Lett. **7,** 1022 (2009).